Experimental Investigation on the velocity profile of supply flow in impinging jet ventilation system

Haruna Yamasawa[1*], *Tomohiro* Kobayashi[2], *Toshio* Yamanaka[2], *Narae* Choi[2], *Moe* Koshida[2], *Mathias* Cehlin[3], and *Arman* Ameen[3]

[1]JSPS Research Fellow PD, Faculty of Environmental Science, Kyushu University, Fukuoka, Japan.
[2]Division of Global Architecture, Graduate School of Engineering, Osaka University, Osaka, Japan.
[3]Faculty of Engineering and Sustainable Development, University of Gävle, Gävle, Sweden.

Abstract. Using the impinging jet ventilation system (IJV), it is possible to accomplish high ventilation effectiveness by creating temperature and contaminant stratification within the room. Since the air is supplied toward the floor and directly spreads into the occupied zone at the lower level, it is important to understand the flow feature of supplied jet around the floor. To understand this, the velocity profile of the jet over the floor at the central cross-section was measured using hotwire anemometer under isothermal conditions, and particle image velocimetry (PIV) under isothermal, cooling, and heating conditions. As a result, the obtained velocity profiles at the central cross-section by the hotwire anemometer and PIV are almost the same in the region more than 0.5 m horizontally away from the supply duct. The velocity in the region close to the supply duct was underestimated when using PIV, due to the insufficient entrainment of the seeding tracer. However, its measurement accuracy is assumed to be sufficient for the flow that goes into the occupied zone. In addition, it was also shown that at the central-cross section, the velocity profiles under isothermal and cooling conditions are almost the same.

1 Introduction

Since HVAC occupies a large portion of the energy usage in the building sector, it is important to install a system with high ventilation effectiveness, for example, the impinging jet ventilation system (IJV). In IJV, the air is supplied through the duct toward the floor, and once the air impinges the floor, it moves along the floor (see Fig. 1) until the air is warmed up by the heat sources. The indoor environment with IJV under both cooling and heating conditions have been studied in terms of ventilation effectiveness in the previous works [1–3]. On the other hand, the studies about the flow feature of the impinging jet along the floor [1,4–6] are still limited, even though this jet plays an important role in this system. A more detailed experimental investigation is required to fully understand the jet flow features. Therefore, a full-scale experiment is conducted to obtain the velocity profiles of the impinging jet, and the results are to be discussed in the present paper.

2 Methods

To understand the flow feature of the supplied jet in IJV, the velocity profile of the jet along the floor is measured under isothermal, cooling, and heating condition. To obtain a detailed and accurate velocity profile, the hotwire anemometer was chosen for the measurement under the isothermal condition. However, because of the limitation of this equipment under non-isothermal conditions, the particle image velocimetry (PIV) was chosen for the measurement under non-isothermal conditions, i.e., cooling and heating conditions. In order to verify the accuracy of PIV, the PIV measurement was also conducted under isothermal conditions. The results of hotwire anemometer and PIV under isothermal conditions will be compared and discussed in the results and discussion section.

Karimipanah et al. [1] reported that velocity profile varies depending on the angle from wall, however, the number of measurement points was limited. Therefore, the velocity profiles at the cross-section 0°, 45° and 90° from the centre of the duct are measured by hotwire anemometer.

The general room setups, the measurement methods of hotwire anemometer and PIV are described in Sections 2.1, 2.2 and 2.3, respectively.

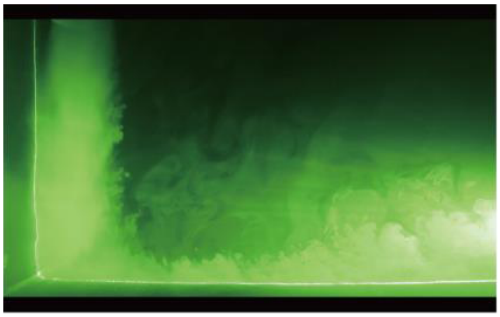

Fig. 1. Visualized jet flow along the floor.

* Haruna Yamasawa: yamasawa@eee.kyushu-u.ac.jp

2.1 General room setups

The measurement was conducted in an experimental chamber with a dimension of 5.00 × 5.45 × 2.77 m shown in Fig. 2. As shown in the figure, there was another chamber (OC: outdoor chamber) next to the target chamber, which is for simulating the heat loss through the external wall. The air inside OC is warmed up under the cooling conditions, cooled down under the heating conditions, and air-conditioning system was turned off under isothermal conditions. The wall between target chamber and OC is not insulated, whereas all the other walls are insulated. The air temperature within OC was controlled by two air conditioners and four fans inside OC. An inlet duct with a diameter of 0.15 m waas mounted at the middle of the wall on the OC-side, 0.6 m above the floor; an outlet is mounted almost in the middle of the ceiling.

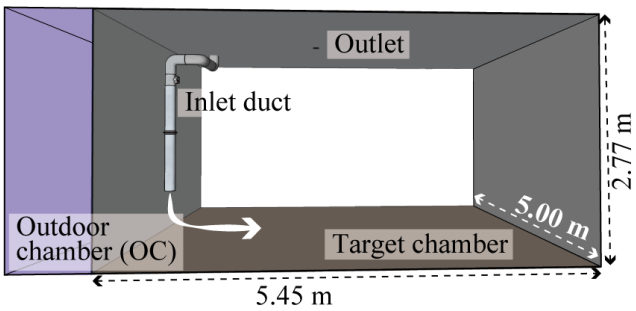

Fig. 2. Setups of the experimental chamber.

The experimental settings are summarised in Table 1. The air-conditioned air is supplied through the inlet duct with a ventilation rate of 178 m^3/h, which accounts for the inlet mean velocity of 2.8 m/s. The airflow rate is measured by an ultrasonic flow meter. The inlet air temperature is controlled at 22 °C, 20 °C, and 30 °C under isothermal, cooling, and heating conditions.

Table 1. The temperature setting of each condition.

	Isothermal	Cooling	Heating
Inlet air	22.0 °C	20.0 °C	30.0 °C
OC air	19.6 °C	35.6 °C	13.4 °C
External air	6.7 °C	4.7 °C	5.5 °C

2.2 Hotwire anemometer

The measurement was first conducted using an I-type hotwire anemometer, where the obtained velocity is the composite velocity of two velocity components. The measurement was conducted at the frequency of 1.0 kHz, and the data was stored in a data logger at the same frequency.

The measurement points of the hotwire anemometer are shown in Fig. 3. The measurement was conducted at 0.2 to 1.0 m from the centre of the inlet duct in the radial direction, whereas the measurement points are set from 0.2 mm to 200 mm above the floor in the vertical direction. Additionally, the velocity profiles were measured in the planes where 0°, 45°, and 90° from the central cross-section of the test chamber, and here, the planes are to be called Plane-00, Plane-45, and Plane 90, respectively.

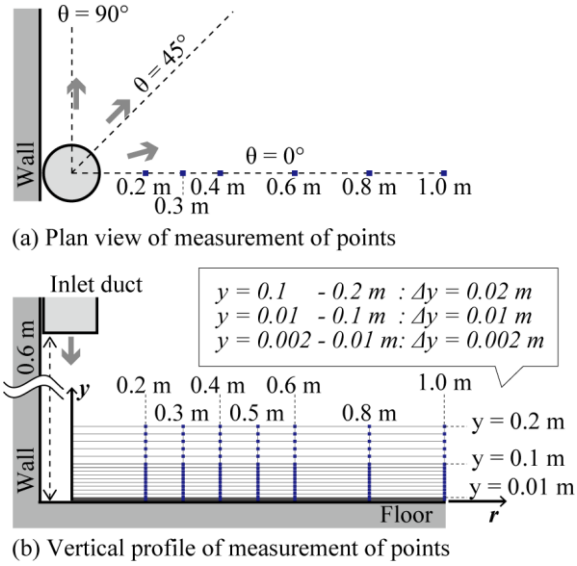

Fig. 3. Measurement points for hotwire anemometer.

2.3 Particle image velocimetry (PIV)

The measurement setups of PIV are shown in Fig. 4. The camera of the PIV system needs to be close to the filming region to obtain the detailed velocity profile

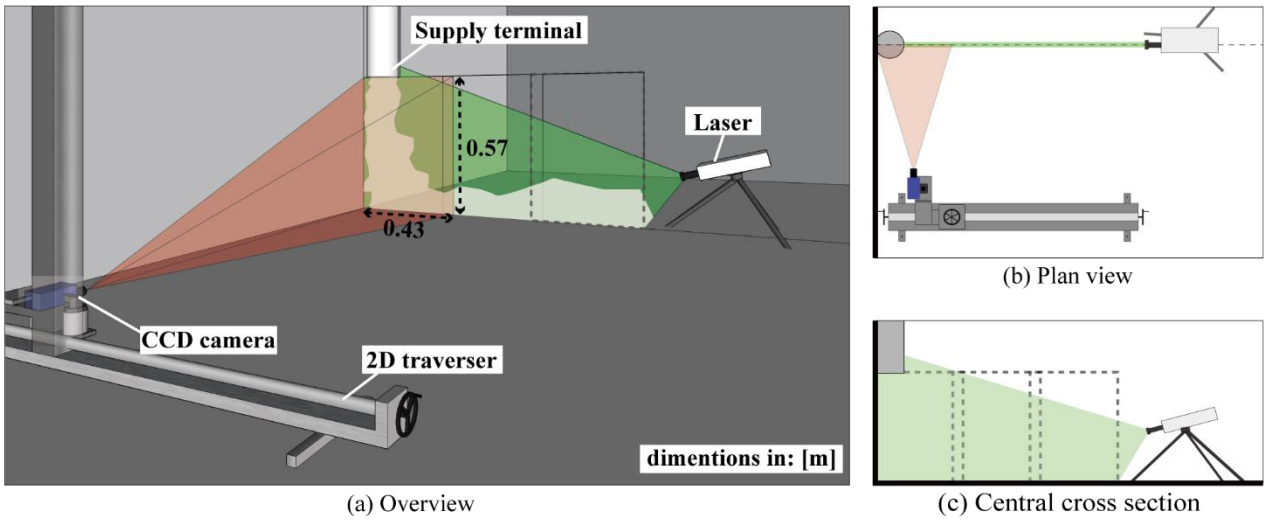

Fig. 4. Setups of PIV measurement.

around the floor, however, it also leads to smaller filming coverage. To obtain the jet flow profiles along the floor from the vicinity of the inlet to 1.0 m away from the inlet duct centre, the measurement is conducted at three positions as shown in the figure, and the results are connected at the end.

Table 2 gives a summary of the PIV measurement method. The double-pulse laser sheets were irradiated at the same time as the photo shoot. Two photos were captured with a time interval of 2.0 × 10^{-3} s, corresponding the double-pulse laser interval, and the instantaneous velocity profile is analysed based on these two photos. The direct cross-correlation method [7] was applied for the analysis with the recursive correlation technique. By detecting a correlation peak within each interrogation window and averaging instantaneous velocity components calculated from a spatial shift within a known time interval, a 2-D time-average velocity distribution was obtained. This data set was sampled every 0.1 s (frequency = 10 Hz) for 10 s. This process was repeated for six times and the mean velocity profile was obtained by averaging this result of 60 s in total. As for the seeding, smoke was generated above the jet so that the jet could induce the smoke.

Table 2. PIV measurement method.

Camera frame size	1,600 pixel × 1,200 pixels
Filming coverage	Approx. 0.57 × 0.43 m
Lase output	50 mJ/pulse
Sampling frequency	10 Hz
Sampling time	10 s × 6 times = 60 s in total
Time interval	2.0 × 10^{-3} s
Interrogation area	32 × 32 pixels × 2 times
Overlap	50%

3 Results and discussions

The results are discussed from three perspectives. (i) The angles; the velocity profiles in the plane that has different angles from the central cross-section are compared in Section 3.1. (ii) the measurement method; the velocity profiles obtained by different measurement methods are discussed in Section 3.2. (iii) The temperature settings; the effect of the temperature setting on the velocity profiles is discussed in Section 3.3.

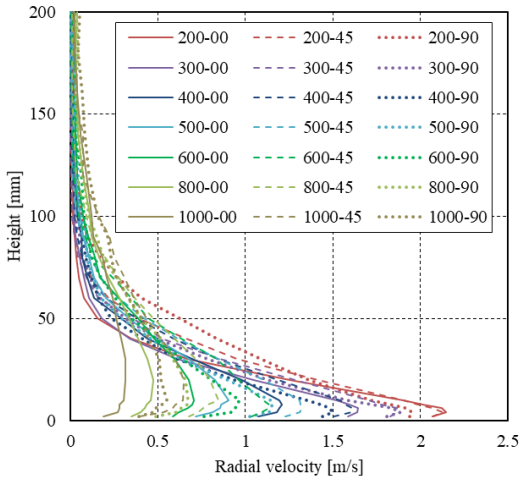

Fig. 5. Vertical profile of radial velocity.

3.1 Planes in different angles

The vertical profiles of radial velocity in Plane-0, Plane-45, and Plane-90 are shown in Fig. 5. As the jet moves along the floor, the maximum velocity decays and the jet width stretches, which is widely known as the turbulent jet flow feature [8]. This feature was identical regardless of the angle. It is also shown that the maximum velocity decay and jet width stretch is significant at Plane-00 than other planes.

To clearly illustrate the difference by angle, the maximum velocity and the jet half width are shown as the correlation with the radial coordinate in Fig. 6 and Fig. 7, respectively. It was shown that the velocity decay and jet width stretch was significant at Plane-00 when compared with other planes. However, when comparing the maximum velocity decay in Plane-45 and Plane-90, the decay was faster in Plane-45, therefore, it is assumed that there is some threshold at the angle between 45° and 90°. On the other hand, the difference in the stretch of the jet half-width is not significant among 45° and 90°.

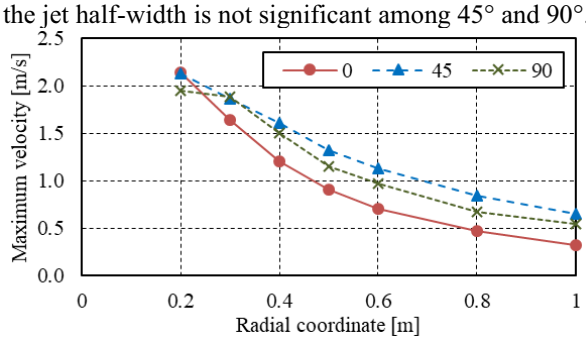

Fig. 6. The correlation between maximum velocity and radial coordinate.

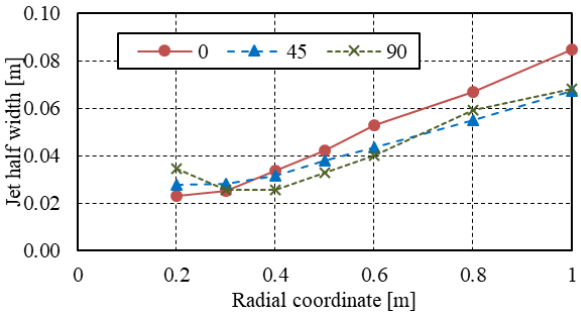

Fig. 7. The correlation between jet half width and radial coordinate.

Finally, the vertical profiles of radial velocity are shown in the dimensionless form in Fig. 8. The jet half-width (height) and maximum radial velocity are used for the reference of the height and radial velocity, respectively. As shown in the figure, it is shown that the correlation can be expressed by an equation regardless of the angle. Verhoff et al. [9] introduced an equation to express the velocity profile of a jet along walls (Eq. (1)). On the other hand, he also claimed that this profile can be roughly expressed by more simple equation for free turbulent jet (Eq. (2)). However, it has to be noted that when comparing these two equations, the velocity at the vicinity of walls is completely different, therefore, this simple equation for free turbulent jet (Eq. (2)) cannot be used when discussing about the velocity at the vicinity of wall.

$$\frac{V}{V_m} = 1.48\left(\frac{y}{b}\right)^{1/7}\left[1 - erf\left(0.678 \times \frac{y}{b}\right)\right] \quad (1)$$

$$\frac{V}{V_m} = exp\left[-C \times \left(\frac{y}{b}\right)^2\right] \quad (2)$$

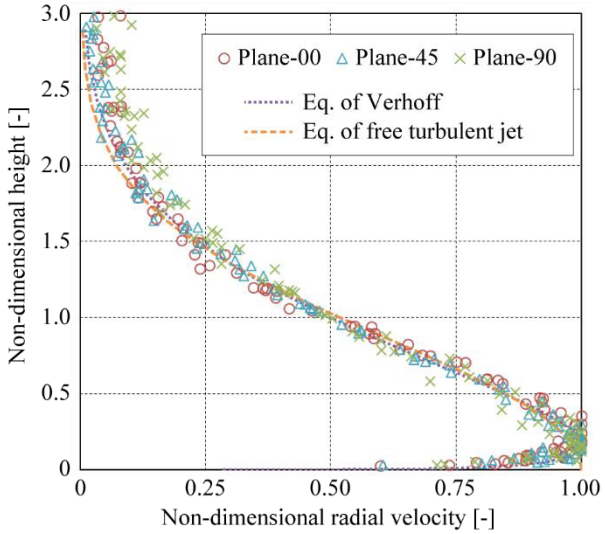

Fig. 8. Dimensionless vertical profile of radial velocity.

3.2 Difference by measurement method

The velocity contours under isothermal conditions in the central cross-section obtained by the hotwire anemometer and PIV are compared in Fig. 9. By using PIV, it is possible to obtain the detailed velocity distribution, however, the air velocity under the inlet duct is small because there was not sufficient tracer.

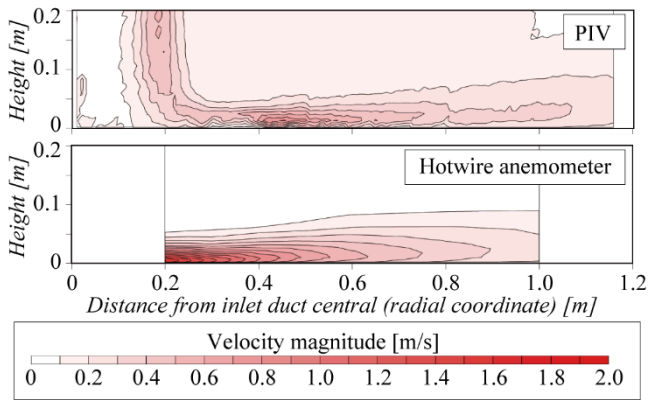

Fig. 9. Comparison of hotwire anemometer and PIV: velocity magnitude distribution in the central cross-section.

The vertical profiles of radial velocity obtained by the hotwire anemometer and PIV in the central cross-section are compared in Fig. 10. As for PIV, the maximum radial velocity in up to the radial coordinate of 0.2 m is significantly different. Since the air in this region has a high velocity and was within the core of the jet, therefore, it is assumed that the surrounding air, which includes the traces, cannot be entrained by the jet into this region. On the other hand, the PIV results in the region from the radial distance of 0.5 to 1.0 m from the inlet centre are almost the same as that of hotwire anemometer. Thus, the PIV with present setups can be used for obtaining the velocity profiles where far enough from the inlet, i.e., where the entrainment of the surrounding air occurs.

3.3 Influence of temperature settings

The distributions of velocity vectors under isothermal, cooling, and heating conditions in the central cross-section obtained by the PIV are compared in Fig. 10. It is shown that the mainstream of the jet stayed around the floor in the present measurement region regardless of the temperature. In terms of the velocity magnitude, the air velocity around the floor under isothermal and heating conditions are almost identical, whereas the velocity is relatively large under cooling conditions. It is assumed that because of the high density of the cool supplied air, the jet stayed around the floor, which leads to a large flow rate, i.e., large air velocity.

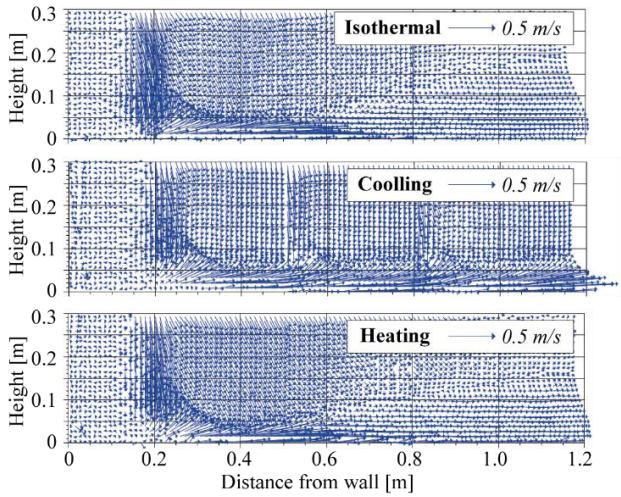

Fig. 10. Velocity vector at the central cross-section (top: isothermal, middle: cooling, and bottom: heating).

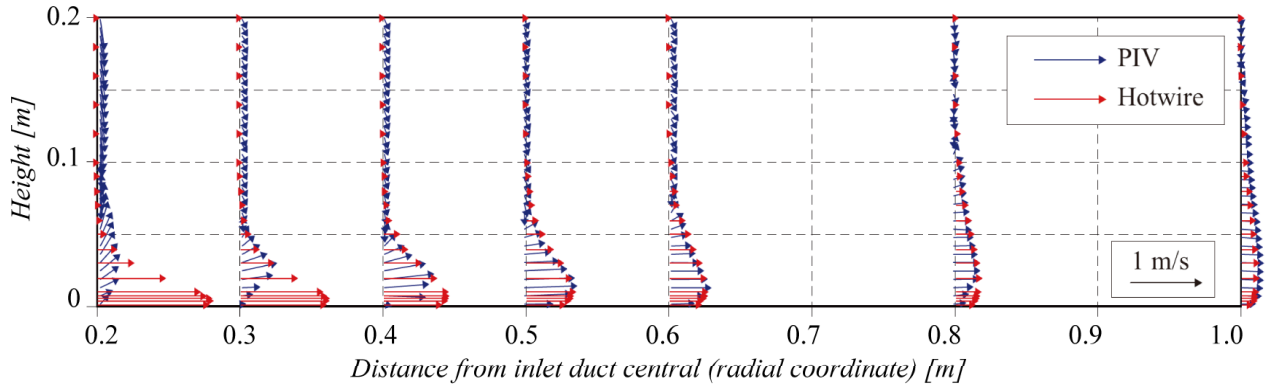

Fig. 11. Comparison of hotwire anemometer and PIV: vertical profiles of radial velocity in the central cross-section.

4 Conclusion

Since the main feature of the IJV is the impinging jet along the floor, therefore, the velocity profiles were measured by the full-scale experiment. The hotwire anemometer and PIV were adopted for the measurement. The measurement under isothermal condition was conducted by both hotwire anemometer and PIV, while the measurement under non-isothermal conditions was conducted only by PIV. In addition, the velocity profiles at the planes with different angle from the central cross-section was measured by the hotwire anemometer.

The results are discussed in terms of (i) the difference of velocity profiles in the planes with several angles from the central cross section; (ii) the difference of measurement results by the hotwire anemometer and PIV; and (iii) the influence of the temperature settings on the velocity profiles.

(i) Different angles

The maximum velocity decay and jet half width stretch differed depending on the angle. Plane-90 (the plane that 90° from the central cross section) was very close to the wall, thus, it was strongly affected by the wall, however, when the height and velocity was expressed by non-dimensional form, the velocity profiles can be expressed by an equation regardless of the angle.

(ii) Measurement method

Because of the flow feature of IJV and the seeding method of tracer, the measurement accuracy of PIV was lower at the region close the inlet. However, the result of the hotwire anemometer and PIV were almost the same at the region 0.5 m away from the inlet duct centre.

(iii) Temperature settings

The main stream of the impinging jet moved along the floor regardless of the temperature settings, however, the velocity magnitude was relatively large under the cooling condition.

This study has the limitation for the inlet velocity, temperature, and geometrical configuration (discharge height and diameter and shape of duct). In addition, since the accuracy of PIV measurement rely on how to seed the tracer, therefore, the seeding method needs to be more improved. However, by using this measurement results, it is possible to validate the results by using computational fluid dynamics. After obtaining a validated CFD model based on the experimental measurement, a more detailed CFD simulation including the evaluation of ventilation effectiveness, can be done as the next step.

References

[1] T. Karimipanah, H.B. Awbi, Theoretical and experimental investigation of impinging jet ventilation and comparison with wall displacement ventilation, Build. Environ. 37 (2002) 1329–1342. https://doi.org/10.1016/S0360-1323(01)00117-2.

[2] H. Yamasawa, T. Kobayashi, T. Yamanaka, N. Choi, M. Cehlin, A. Ameen, Effect of supply velocity and heat generation density on cooling and ventilation effectiveness in room with impinging jet ventilation system, Build. Environ. 205 (2021) 108299. https://doi.org/10.1016/j.buildenv.2021.108299.

[3] X. Ye, Y. Kang, F. Yang, K. Zhong, Comparison study of contaminant distribution and indoor air quality in large-height spaces between impinging jet and mixing ventilation systems in heating mode, Build. Environ. 160 (2019) 106159. https://doi.org/10.1016/j.buildenv.2019.106159.

[4] J. Varodoumpun, M. Navvab, The impact of terminal configurations in impinging jet ventilated room, IAQVEC 2007 Proc. - 6th Int. Conf. Indoor Air Qual. Vent. Energy Conserv. Build. Sustain. Built Environ. 3 (2007) 389–396.

[5] A. Ameen, M. Cehlin, U. Larsson, H. Yamasawa, T. Kobayashi, Numerical Investigation of the Flow Behavior of an Isothermal Corner Impinging Jet for Building Ventilation, Build. Environ. 223 (2022) 109486. https://doi.org/10.1016/j.buildenv.2022.109486.

[6] H.J. Chen, B. Moshfegh, M. Cehlin, Numerical investigation of the flow behavior of an isothermal impinging jet in a room, Build. Environ. 49 (2012) 154–166. https://doi.org/10.1016/j.buildenv.2011.09.027.

[7] H. Kotani, T. Kobayashi, Accuracy verification of processing methodology in particle image velocimetry for flow around building, J. Environ. Eng. (Transactions AIJ). 80 (2015) 741–749. https://doi.org/10.3130/aije.80.741.

[8] N. Rajaratnam, Turbulent Jets, Elsevier Science Ltd., Amsterdam, 1976.

[9] A. Verhoff, The two-dimensional, turbulent wall jet with and without an external free stream, 1963. https://apps.dtic.mil/sti/citations/AD0406073.